Progress In Electromagnetics Research, Vol. 113, 111–126, 2011

SYNTHESIS OF MULTI-STEP COPLANAR WAVEGUIDE-TO-MICROSTRIP TRANSITION

S. Costanzo

Dipartimento di Elettronica, Informatica e Sistemistica
University of Calabria, Via P. Bucci, Rende (CS) 87036, Italy

Abstract—A synthesis procedure is developed in this paper for the design of N-step coplanar waveguide-to-microstrip transitions. An equivalent circuit approach is adopted to model the structure in terms of N cascaded $ABCD$ matrices relative to the N coplanar waveguide sections forming the transition. A constrained optimization problem is formulated as the minimum finding of a proper functional to accurately determine the transition dimensions by imposing an upper bound to the return loss within a prescribed frequency band. An iterative N-step procedure is developed to find the optimization problem solution. Numerical results on millimeter-wave transition configurations are provided to demonstrate the effectiveness of the proposed synthesis method. A back-to-back transition prototype with $N = 3$ sections is then fabricated and characterized in terms of measured S-parameters to experimentally demonstrate a return loss better than 10 dB in the frequency range from 1 GHz up to 40 GHz.

1. INTRODUCTION

The coplanar waveguide (CPW) configuration offers significant advantages and flexibility in the design of hybrid and monolithic microwave integrated circuits, especially when working at millimeter and sub-millimeter frequency ranges. As compared to standard microstrip lines, it provides small radiation loss, low dispersion, simple integration of active and passive devices, and also it eliminates the need for via holes [1]. The conventional CPW [1] consists of a center strip conductor and two ground planes on both sides, which are made of finite extent in practical circuits. The CPW configuration with additional backside grounding, commonly called

Received 29 November 2010, Accepted 24 January 2011, Scheduled 28 January 2011
Corresponding author: Sandra Costanzo (costanzo@deis.unical.it).

conductor-backed coplanar waveguide, provides further advantages in terms of mechanical stability, thermal dissipation capability and integration. The above features make CPW and its variant conductor-backed CPW ideally suited for the design of low-loss, compact and inexpensive uniplanar structures [2–4]. Applications involving the integration of CPWs and microstrip lines on the same circuit or adopting on-wafer measurement techniques with CPW probes require the flexible combination and compatibility of both microstrip and CPW technologies. As a consequence of this, the design of wideband, low-loss and reduced size transitions between CPWs and microstrip lines has become an essential point, subject to rigorous research since many years [5–10]. When working at millimeter-wave frequencies, the requirement of a transition structure is also related to the dimensions limitations of standard connectors, often preventing a direct connection to CPWs circuits. An interesting transition structure which provides a gradual transformation of the electric and magnetic fields between a CPW or conductor-backed CPW and a microstrip or a stripline was proposed in [11, 12]. It exploits results coming from the analysis of normal propagation modes in conductor-backed CPW structures [13, 14] to assume the characteristic impedance of conductor-backed CPW as given by the combination of two characteristic impedances associated to the CPW mode and the microstrip mode, respectively. These impedances are strongly influenced by the conductor-backed CPW parameters dimensions. In particular, for small values of the ratio between the center line-to-ground line separation and the substrate height, the CPW propagation mode is dominant. On the other hand, when this ratio increases, the conductor-backed CPW structure turns to a microstrip line and the microstrip mode becomes more dominant. On the basis of this consideration, the configuration presented in [11, 12] realizes a smooth transition, in terms of both impedance and field match, by gradually enlarging the width of the center line of conductor-backed CPW to the microstrip width, while keeping the characteristic impedance value constant along the structure. For simplicity of implementation, the transition is divided into N sections of conductor-backed CPW having equal length and impedance, with the geometrical parameters of each section derived from the structural expressions reported in [1]. A numerical analysis based on the use of Ansoft HFSS simulator is presented in [11, 12] to demonstrate the wideband behavior of the transition structure, by examining the effect of the length as well as the number of sections on the operating bandwidth. Experimental results on back to back transitions are also discussed in [11, 12] to validate the proposed transition configuration.

In this paper, a synthesis procedure is developed to accurately determine the dimensions of the conductor-backed CPW-to-microstrip transition configuration proposed in [11, 12]. Based on the approach outlined in [11, 12], the fundamental mode propagation is assumed, and each section of the conductor-backed CPW-to-microstrip transition is properly dimensioned to prevent the excitation of higher-order modes [15, 16] within the operating frequency band. A gradual smooth transformation is realized from the CPW mode to the microstrip mode, while keeping the characteristic impedance constant along the transition [12], so reflections due to impedance changes are avoided and the assumption of single-mode operation gives accurate results. As a matter of fact, it is expected only that reactive phenomena responsible for resonances could be produced at the transition sections due to dimensions changes. On the basis of single-mode assumption, a simplified equivalent circuit approach is adopted, with the transition structure modelled in terms of N cascaded $ABCD$ matrices relative to its N sections, and a compact expression is derived for the reflection coefficient S_{11} at the transition input as a function of the propagation constants of the N conductor-backed CPW transition sections. By imposing a proper upper bound to the return loss within a frequency band limited by the intersection frequency between the fundamental mode and the first higher-order mode, a constrained optimization problem is formulated as the minimum finding of a N variable functional, and an iterative N-step procedure is developed to find the solution in terms of the N phase constants relative to the N transition sections. The structural formulas of conductor-backed CPWs are finally applied to determine the N-step transition dimensions. The effectiveness of the synthesis procedure is demonstrated by discussing numerical results on two millimeter-wave conductor-backed CPW-to-microstrip transition configurations with different number of sections, and validation with Ansoft Designer simulations are provided. For both the examined transition structures, a wideband behavior is numerically predicted, with a return loss below -10 dB from 1 GHz up to 65 GHz. Furthermore, experimental validations are provided in terms of measured S-parameters on a back-to-back 3-step transition prototype, by confirming the correct operating behavior of the return loss up to 40 GHz.

2. THEORY

The conductor-backed CPW-to-microstrip transition proposed in [11, 12] and examined in this paper is shown in Fig. 1. It is used to connect a conductor-backed CPW of dimensions W_c, S_c, G_c

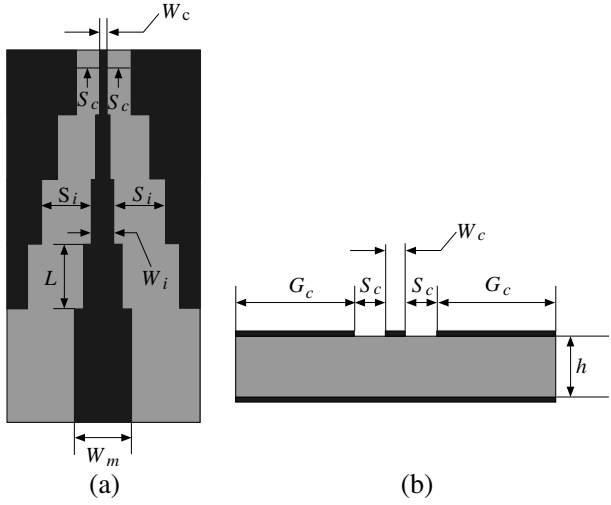

Figure 1. Layout of conductor-backed CPW-to-microstrip transition: (a) Top view and (b) Side view.

to a microstrip line of width W_m, and consists of N sections of conductor-backed CPW with equal length L and parameters W_i, S_i $(i = 1, 2, \ldots, N)$. Each section is designed to have a characteristic impedance Z_c, while Z_o is the impedance value of the connected conductor-backed CPW and microstrip line. To guarantee the gradual change of the electric and magnetic fields from the CPW mode to the microstrip mode, the proper design of the transition in Fig. 1 leads to increase the parameters W_i, $S_i\,(i = 1, 2, \ldots, N)$ along the structure, from the conductor-backed CPW side to the microstrip line. In [11, 12], this design process is performed uniquely on the basis of parametric simulations on Ansoft HFSS software, with no specific criteria to determine the structure dimensions, so implying a heavy repeatition procedure, with variable simulation costs when changing the design constraints in terms of operating frequency band and dimensions. In this paper, a theoretical modelling of the structure in Fig. 1 is developed by assuming the equivalent circuit of Fig. 2, where the connected conductor-backed CPW and the microstrip line are both described by uniform transmission lines of characteristic impedance Z_o (Fig. 2(a)), and the transition is modelled in terms of N cascaded $ABCD$ matrices (Fig. 2(b)) relative to the N sections of uniform transmission lines having characteristic impedance Z_c.

The two-port $ABCD$ matrix elements of the ith section are given

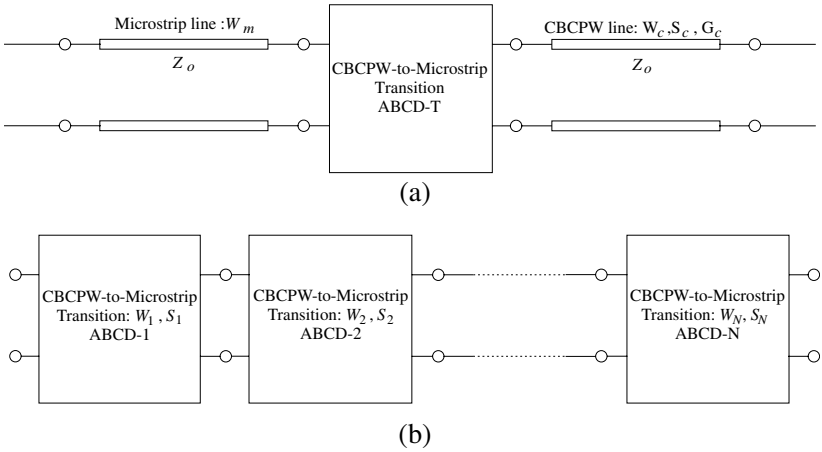

Figure 2. Equivalent circuit topology of conductor-backed CPW-to-microstrip transition: (a) Full cascaded circuit and (b) Cascaded circuit of N-step transition.

by [17]:

$$ABCD_i = \begin{bmatrix} \cosh \gamma_i L & Z_c \sinh \gamma_i L \\ \frac{1}{Z_c} \cdot \sinh \gamma_i L & \cosh \gamma_i L \end{bmatrix} \tag{1}$$

where $\gamma_i = \alpha_i + j\beta_i$ is the complex propagation constant, with:

$$\beta_i = \beta_o \sqrt{\epsilon_{eff}^i} \tag{2}$$

β_o being the free-space propagation constant.

The attenuation constant α_i and the effective dielectric constant ϵ_{eff}^i of the ith section are determined by the quasi-static formulas based on the conformal mapping technique [1].

The $ABCD$ matrix of the entire transition is derived by cascading the $ABCD$ matrices relative to all sections, so giving:

$$ABCD_T = \begin{bmatrix} A_T & B_T \\ C_T & D_T \end{bmatrix} = \prod_{i=1}^{N} \begin{bmatrix} A_i & B_i \\ C_i & D_i \end{bmatrix} \tag{3}$$

Some manipulations lead to obtain:

$$A_T = D_T = \cosh \left[\left(\gamma_1 - \sum_{i=2}^{N} \gamma_i \right) L \right]$$

$$B_T = Z_c \sinh \left[\left(\gamma_1 + \sum_{i=2}^{N} \gamma_i \right) L \right]$$

$$C_T = \frac{1}{Z_c} \cdot \sinh\left[\left(\gamma_1 + \sum_{i=2}^{N} \gamma_i\right) L\right] \tag{4}$$

The reflection coefficient S_{11} at the transition input can be expressed in terms of $ABCD_T$ parameters as follows [17]:

$$S_{11} = \frac{A_T + \frac{B_T}{Z_o} - C_T Z_o - D_T}{A_T + \frac{B_T}{Z_o} + C_T Z_o + D_T} \tag{5}$$

The substitution of expressions (4) into relation (5) gives:

$$S_{11} = \frac{\left(\frac{Z_c^2 - Z_o^2}{Z_c^2 + Z_o^2}\right) \cdot \sinh\left[\left(\gamma_1 + \sum_{i=2}^{N} \gamma_i\right) L\right]}{\sinh\left[\left(\gamma_1 + \sum_{i=2}^{N} \gamma_i\right) L\right] + \frac{2Z_c Z_o}{Z_c^2 + Z_o^2} \cosh\left[\left(\gamma_1 - \sum_{i=2}^{N} \gamma_i\right) L\right]} \tag{6}$$

A compact form of expression (6) can be written as:

$$S_{11} = P \cdot \frac{\sinh\left(\theta_1 + \sum_{i=2}^{N} \theta_i\right)}{\sinh\left(\theta_1 + \sum_{i=2}^{N} \theta_i\right) + Q \cosh\left(\theta_1 - \sum_{i=2}^{N} \theta_i\right)} \tag{7}$$

where:

$$P = \frac{Z_c^2 - Z_o^2}{Z_c^2 + Z_o^2}, \quad Q = \frac{2Z_c Z_o}{Z_c^2 + Z_o^2}, \quad \theta_i = \gamma_i L, \quad i = 1, 2, \ldots, N \tag{8}$$

Following Fano's considerations on the theoretical limitations of broadband matching [18], we can impose the magnitude of the reflection coefficient S_{11} to be smaller than or equal to a specified value ρ_m within a prescribed frequency band B, i.e.:

$$|S_{11}(f)| \leq \rho_m, \quad \forall f \in B \tag{9}$$

Due to the assumption of fundamental mode propagation, the reliable band B of the approach adopted in the paper is upper limited by the intersection frequency between the fundamental mode and the first higher-order mode [15, 16]. However, this upper bound does not give strong limitations, as a proper selection of CPW dimensions can inhibit higher-order modes, so providing a very wideband behavior.

By substituting expression (7) into relation (9), we have:

$$\left| \frac{\sinh(\theta_1 + \sum_{i=2}^{N} \theta_i)}{\sinh(\theta_1 + \sum_{i=2}^{N} \theta_i) + Q \cosh(\theta_1 - \sum_{i=2}^{N} \theta_i)} \right| \leq \frac{\rho_m}{|P|} \tag{10}$$

The application of Schwarz's inequality [19] gives:

$$\left|\sinh\left(\theta_1+\sum_{i=2}^{N}\theta_i\right)+Q\cosh\left(\theta_1-\sum_{i=2}^{N}\theta_i\right)\right|$$
$$\leq \left|\sinh\left(\theta_1+\sum_{i=2}^{N}\theta_i\right)\right|+Q\left|\cosh\left(\theta_1-\sum_{i=2}^{N}\theta_i\right)\right| \tag{11}$$

from which:

$$\frac{\left|\sinh\left(\theta_1+\sum_{i=2}^{N}\theta_i\right)\right|}{\left|\sinh\left(\theta_1+\sum_{i=2}^{N}\theta_i\right)\right|+Q\left|\cosh\left(\theta_1-\sum_{i=2}^{N}\theta_i\right)\right|}\leq\frac{\rho_m}{|P|} \tag{12}$$

Let us impose:

$$\theta_1-\sum_{i=2}^{N}\theta_i=a_1+jb_1,\quad \theta_1+\sum_{i=2}^{N}\theta_i=a_2+jb_2 \tag{13}$$

where:

$$a_1=\left(\alpha_1-\sum_{i=2}^{N}\alpha_i\right)L,\quad b_1=\left(\beta_1-\sum_{i=2}^{N}\beta_i\right)L \tag{14}$$

$$a_2=\left(\alpha_1+\sum_{i=2}^{N}\alpha_i\right)L,\quad b_2=\left(\beta_1+\sum_{i=2}^{N}\beta_i\right)L \tag{15}$$

In the case of small losses ($\alpha_i \ll \beta_i, \forall i = 1, 2, \ldots, N$), we can assume $a_1 \simeq 0$ and $a_2 \simeq 0$, so a compact form of relation (12) can be easily derived as:

$$C_1|\sin b_2| \leq C_2|\cos b_1| \tag{16}$$

where

$$C_1=\left(1-\frac{\rho_m}{|P|}\right),\quad C_2=\frac{\rho_m Q}{|P|} \tag{17}$$

The unknowns $\beta_i(f)$ ($f \in B, i = 1, 2, \ldots, N$) into Eq. (16) are determined as solutions of a nonlinearly constrained optimization problem [20], formulated as the finding of the least value of the functional:

$$\psi(\beta_1, \beta_2, \ldots, \beta_N) = C_1|\sin b_2| - C_2|\cos b_1| \tag{18}$$

subject to the constraint given by Eq. (2).

From the knowledge of the phase constant β_i relative to the ith section, the effective dielectric constant ϵ^i_{eff} is derived, which in turns is related to the section dimensions W_i, S_i by the expression [1]:

$$\epsilon^i_{eff} = \frac{1 + \epsilon_r \cdot \frac{K(k')}{K(k)} \cdot \frac{K(k_1)}{K(k'_1)}}{1 + \frac{K(k')}{K(k)} \cdot \frac{K(k_1)}{K(k'_1)}} \tag{19}$$

where $k = \frac{a}{b}$, $k_1 = \frac{\tanh(\frac{\pi a}{4h})}{\tanh(\frac{\pi b}{4h})}$, $k' = \sqrt{1-k^2}$, $k'_1 = \sqrt{1-k_1^2}$, $a = W_i$, $b = W_i + 2S_i$, $K(\ldots)$ being the complete elliptic integral of the first kind.

To solve the problem, an iterative N-step optimization procedure is performed, for a given number N of sections. Due to the small changes between adjacent sections, we assume, as initial guess, all β_i are equal, so that:

$$b_1 = -(N-2)\beta_1, \quad b_2 = N\beta_1 \tag{20}$$

By substituting relations (20) into Eq. (18), the functional to be minimized at the first step with respect to the single variable β_1 can be expressed as:

$$\psi_1(\beta_1) = C_1 \left|\sin\beta_1 \cdot U_{N-1}(\cos\beta_1)\right| - C_2 \left|T_{N-2}(\cos\beta_1)\right| \tag{21}$$

where $T_j(\ldots)$ and $U_j(\ldots)$ are the Chebyshev polynomials of the first and the second kind, respectively, and order j [19].

At the second step, the terms b_1, b_2 are expressed as:

$$b_1 = \beta_1 - (N-1)\beta_2, \quad b_2 = \beta_1 + (N-1)\beta_2 \tag{22}$$

Relations (22) are substituted into Eq. (18) for defining the second-step functional to be minimized with respect to the unknown β_2, namely:

$$\begin{aligned}\psi_2(\beta_2) \;=\; & C_1 \left|\sin\beta_1 \cdot [T_{N-1}(\cos\beta_2) + \cos\beta_1 \cdot U_{N-2}(\cos\beta_2)]\right| \\ & -C_2 \left|\cos\beta_1 \cdot T_{N-1}(\cos\beta_2) + \sin^2\beta_2 \cdot U_{N-2}(\cos\beta_2)\right| \end{aligned} \tag{23}$$

At the generic nth step, the optimization procedure involves the finding

of the least value of the functional:

$$\begin{aligned}\psi_n(\beta_n) \;=\; & C_1 \left| \sin\left(\sum_{i=1}^{n-1}\beta_i\right)\cdot T_{N-n+1}(\cos\beta_n) \right. \\ & \left. +\cos\left(\sum_{i=1}^{n-1}\beta_i\right)\cdot\sin\beta_n\cdot U_{N-n}(\cos\beta_n)\right| \\ & -C_2\left|\cos\left(\beta_1-\sum_{i=2}^{n-1}\beta_i\right)\cdot T_{N-n+1}(\cos\beta_n)\right. \\ & \left. +\sin\left(\beta_1-\sum_{i=2}^{n-1}\beta_i\right)\cdot U_{N-n}(\cos\beta_n)\right| \end{aligned} \tag{24}$$

Finally, at the Nth step, the functional to be minimized is expressed as:

$$\begin{aligned}& \psi_N(\beta_N) \\ =\; & C_1\left|\sin\left(\sum_{i=1}^{N-1}\beta_i\right)\cdot\cos\beta_N+\cos\left(\sum_{i=1}^{N-1}\beta_i\right)\cdot\sin\beta_N\right. \\ & \left. -C_2\left|\cos\left(\beta_1-\sum_{i=2}^{N-1}\beta_i\right)\cdot\cos\beta_N+\sin\left(\beta_1-\sum_{i=2}^{N-1}\beta_i\right)\cdot\sin\beta_N\right|\end{aligned} \tag{25}$$

Once solved the optimization problem with respect to the unknowns β_i $(i = 1, 2, \ldots, N)$, the effective dielectric constant ϵ_{eff}^i of each section is obtained from Eq. (2) and the dimensions W_i, S_i are determined as solutions of Eq. (19) which satisfy the physical realizability constraints of the structure, namely:

$$\begin{aligned} & W_c \le W_i \le W_m \\ & S_i > S_c \\ & W_i > W_{i-1}, \quad i = 2, 3, \ldots, N \\ & S_i > S_{i-1}, \quad i = 2, 3, \ldots, N \end{aligned} \tag{26}$$

The optimization procedure described above can be summarized as follows:

1. assign the dimensions of the conductor-backed CPW and the microstrip line to be connected, both having the same characteristic impedance Z_o;
2. determine the reliable frequency band B by performing the characterization of higher-order modes relative to the conductor-backed CPW;

3. fix the number N of transition sections, all having the same characteristic impedance Z_1, and a total transition length equal to $\lambda_g/4$, λ_g being the guided wavelength;
4. impose a suitable upper bound ρ_m on the magnitude of the reflection coefficient at the transition input within the reliable band B determined from stage 2;
5. apply the N-step optimization procedure to determine the phase constant of each transition section;
6. from the phase constants obtained in stage 5, determine the effective dielectric constant and the dimensions of the N transition sections which satisfy the physical realizability constraints.

The proposed synthesis approach can have practical applications in the design of CPW-to-microstrip transitions useful to the packaging of compact integrated circuits [20–29].

Even if formulated for the connection between a conductor-backed CPW and a microstrip line, the optimization procedure can be also applied to the case of CPW without back plane, as originally considered in [11, 12], by simply adopting the proper structural formulas [1]. In this case, it is expected that the absence of the back plate will reduce the occurrences of unwanted higher-order modes [15].

3. NUMERICAL RESULTS

The synthesis procedure outlined in the previous section is applied to accurately design two millimeter-wave transitions between a conductor-backed CPW and a microstrip line, both having characteristic impedance $Z_o = 50\,\Omega$ on a dielectric substrate Arlon DiClad 880 ($\epsilon_r = 2.2$ and $\tan\delta = 0.0009$) of height $h = 0.254\,\text{mm}$. On the basis of quasi-static formulas reported in [1], the dimensions of the conductor-backed CPW are selected as $W_c = 0.623\,\text{mm}$, $S_c = 0.1\,\text{mm}$ and $G_c = 3\,\text{mm}$, at a central design frequency $f_o = 30\,\text{GHz}$. The microstrip line has width $W_m = 0.773\,\text{mm}$. To determine the reliable frequency band B, a characterization of the CPW higher-order modes is performed by following the approach outlined in [16], where the resonance effects in both the substrate thickness and the lateral directions are modelled in terms of an effective permittivity ϵ_{eff}^{mn} for each higher-order mode HM_{mn}. In Table 1, the intersection frequency between the ϵ_{eff} curves of the fundamental mode and the generic higher-order mode HM_{mn} is reported for the first three propagating modes in the conductor-backed CPW. It can be observed that the first higher-order mode HM_{01} intersects the fundamental mode at a

frequency equal to 67 GHz, so an operating frequency band B going from 1 GHz up to 65 GHz is imposed.

The synthesis method is applied to design two different transitions, with $N = 3$ and $N = 5$ conductor-backed CPW sections, respectively, all having the same characteristic impedance $Z_c = 51\,\Omega$ slightly different from Z_o. In both cases, an upper bound $\rho_m = -10\,\text{dB}$ is imposed for the magnitude of the reflection coefficient S_{11} at the transition input, and a total length equal to 1.68 mm ($\lambda_g/4$, λ_g being the guided wavelength) is assumed for the transition. A Sequential Quadratic Programming (SQP) procedure based on a constrained quasi-Newton method [30] is applied to solve the N-step optimization problem formulated in Section 2 with respect to the unknowns $\beta_i(f)$ $(i = 1, 2, \ldots, N)$. The effective dielectric constant

Table 1. Intersection frequency f_c between fundamental mode and higher-order modes HM_{mn} for conductor-backed CPW.

Mode	Frequency f_c [GHz]
HM_{01}	67
HM_{02}	133
HM_{10}	890

Table 2. Effective dielectric constant and dimensions of conductor-backed CPW-to-microstrip transition of Fig. 1 (results from synthesis procedure of Section 2 — Case $N = 3$).

Section number	ϵ_{eff}^i	L (mm)	W_i (mm)	S_i (mm)
$i = 1$	1.78	0.56	0.65	0.12
$i = 2$	1.81	0.56	0.7	0.17
$i = 3$	1.83	0.56	0.73	0.23

Table 3. Effective dielectric constant and dimensions of conductor-backed CPW-to-microstrip transition of Fig. 1 (results from synthesis procedure of Section 2 — Case $N = 5$).

Section number	ϵ_{eff}^i	L (mm)	W_i (mm)	S_i (mm)
$i = 1$	1.77	0.336	0.64	0.11
$i = 2$	1.79	0.336	0.67	0.14
$i = 3$	1.81	0.336	0.7	0.17
$i = 4$	1.83	0.336	0.73	0.23
$i = 5$	1.86	0.336	0.76	0.3

ϵ^i_{eff} and the dimensions W_i, S_i retrieved from the synthesis procedure are summarized in Tables 2 and 3 for each section of the two designed transitions with $N = 3$ and $N = 5$, respectively. Each step of the synthesis procedure has required 3 iterations for the minimization of the relative functional.

To demonstrate the effectiveness of the optimization method, the analytical values of the phase constants $\beta_i\,(i = 1, 2, \ldots, N)$ are computed from the synthesized parameters of Tables 2 and 3 by adopting the conformal-mapping expressions reported in [1]. A successful comparison between analytical and synthesized results can be observed under Fig. 3 for the phase constants β_1 (Fig. 3(a)), β_2 (Fig. 3(b)) and β_3 (Fig. 3(c)) relative to the transition with $N = 3$ sections. Analogous results are obtained for the case with $N = 5$ sections.

To verify the satisfaction of constraint (9), the return loss S_{11} is computed from the synthesized phase constants $\beta_i (i = 1, 2, \ldots, N)$ by adopting Eq. (7) under the hyphotesis of small losses, as discussed in Section 2. For both transition configurations, with $N = 3$ and $N = 5$ sections, respectively, the magnitude of the reflection coefficient is correctly below the fixed upper bound $\rho_m = -10\,\text{dB}$ within the

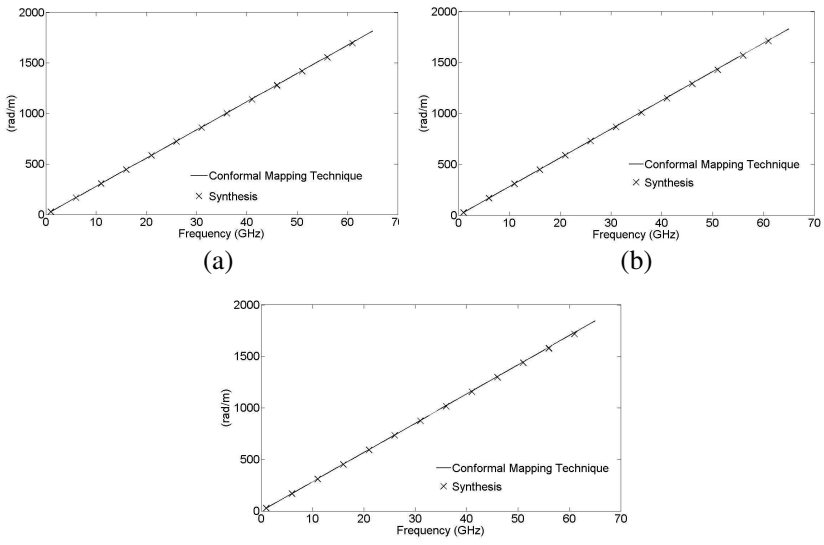

Figure 3. Analytical and synthesized phase constants values for the transition with $N = 3$ sections: (a) β_1, (b) β_2, (c) β_3.

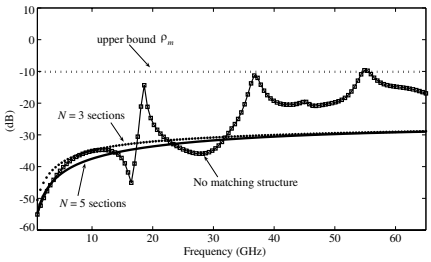

Figure 4. Return loss of conductor-backed CPW-to-microstrip transitions obtained from the synthesis procedure.

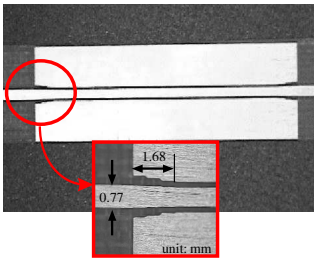

Figure 5. Photograph of back-to-back transition with $N = 3$ sections.

prescribed frequency band going from 1 GHz up to 65 GHz (Fig. 4). In the same Fig. 4, the return loss for the connection with no matching structure is reported for reference.

4. EXPERIMENTAL RESULTS

The experimental validation of the proposed synthesis technique is performed by examining the S-parameters behavior of a back-to-back transition obtained from two cascaded conductor-backed CPW-to-microstrip transitions, with $N = 3$ sections, connected through a uniform conductor-backed CPW line. The two transitions dimensions are those summarized in Table 2, obtained from the N-step optimization procedure discussed in Section 2. A 10 mm length is fixed for the central conductor-backed CPW and the input microstrip lines. A photograph of the back-to-back prototype, realized by conventional photolitography, is illustrated in Fig. 5, where a particular of the $N = 3$ steps transition is also reported. S-parameters measurements are performed by using the Anritsu 37269C network analyzer together with the Anritsu text fixture. Due to the frequency limitations of available instrumentation equipments, well working up to 40 GHz, higher frequencies are excluded from the measurement range. The experimental S-parameters of the back-to-back transition, shown in Figs. 6–7, are found to be in a satisfactory agreement with results obtained from Ansoft Designer simulations (Planar EM simulator), over the frequency range between 1 GHz and 40 GHz, thus confirming the broadband transmission behavior of the designed conductor-backed CPW-to-microstrip transition. In particular, the measured return loss correctly remains below the limit of -10 dB all over the frequency range fixed in the synthesis procedure.

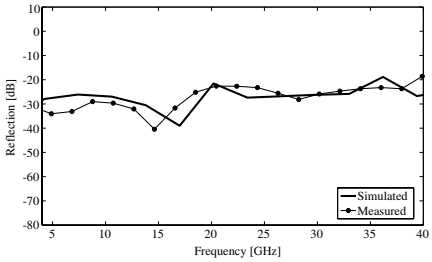

Figure 6. Reflection parameter of back-to-back $N = 3$ sections transition prototype: comparison between simulations and measurements.

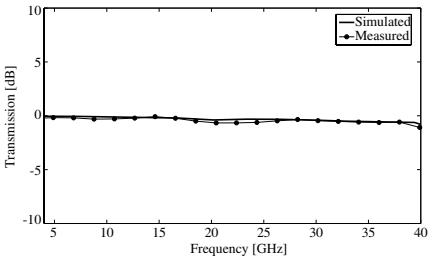

Figure 7. Transmission parameter of back-to-back $N = 3$ setions transition prototype: comparison between simulations and measurements.

REFERENCES

1. Simons, R. N., *Coplanar Waveguide Circuits, Components, and Systems*, Wiley-Interscience, New York, 2001.
2. Zhang, G. M, J. S. Hong, B. Z. Wang, Q. Y. Qin, J. B. Mo, and D.-M. Wan, "A novel multi-folded UWB antenna FED by CPW," *Journal Electromagnetice Waves Applications*, Vol. 21, No. 14, 2109–2119, 2007.
3. Chen, N.-W. and Y.-C. Liang, "An ultra-broadband, coplanar-waveguide FED circular monopole antenna with improved radiation characteristics," *Progress In Electromagnetics Research C*, Vol. 9, 193–207, 2009.
4. Dastranj, A. and M. Biguesh, "Broadband coplanar waveguide-FED wide-slot antenna," *Progress In Electromagnetics Research C*, Vol. 15, 89–101, 2010.
5. Simons, R. N. and R. Q. Lee, "Coplanar-waveguide/Microstrip probe coupler and applications to antennas," *IEE Electronics Letters*, Vol. 26, 1998–2000, 1990.
6. Mirshekar-Syahkal, D., D. J. Newson, D. Wake, and I. D. Henning, "Wide-band transitions for applications in MMIC's and OEIC's," *IEEE Microwave Guided Wave Lett.*, Vol. 4, 299–300, 1994.
7. Dib, N. I. R., N. Simons, and L. P. B. Katehi, "New uniplanar transitions for circuit and antenna applications," *IEEE Trans. Microwave Theory Tech.*, Vol. 43, 2868–2873, 1995.
8. Gauthier, G. P., L. P. Katehi, and G. M. Rebeiz, "W-band finite ground coplanar waveguide (FGCPW) to microstrip line transition," *1998 IEEE MTT-S Int. Microwave Symp. Digest*,

107–109, 1998.

9. Ellis, T. J., J.-P. Raskin, L. P. Katehi, and G. M. Rebeiz, "A wideband CPW-to-microstrip transition for millimeter-wave packaging," *1999 IEEE MTT-S Int. Microwave Symp. Digest*, 629–632, 1999.
10. Raskin, J.-P., G. Gauthier, L. P. Katehi, and G. M. Rebeiz, "Mode conversion at GCPW-to-microstrip-line transitions," *IEEE Trans. Microwave Theory Tech.*, Vol. 48, 158–161, 2000.
11. Safwat, A. M. E., K. A. Zaki, W. Johnson, and C. H. Lee, "Novel design for coplanar waveguide to microstrip transition," *2001 IEEE MTT-S Int. Microwave Symp. Digest*, 607–610, 2001.
12. Safwat, A. M. E., K. A. Zaki, W. Johnson, and C. H. Lee, "Novel transition between different configurations of planar transmission lines," *IEEE Microwave Wireless Comp. Lett.*, Vol. 12, 128–130, 2002.
13. Riaziat, M., I. J. Feng, R. Majidi-Ahy, and B. A. Auld, "Single-mode operation of coplanar waveguides," *IEE Electronics Letters*, Vol. 23, 1281–1283, 1987.
14. Safwat, A. M. E., K. A. Zaki, W. Johnson, and C. H. Lee, "Mode-matching analysis of conductor backed coplanar waveguide with surface etching," *Journal of Electromagnetics Waves and Applications*, Vol. 15, No. 5, 627–641, 2001.
15. Riaziat, M., R. Majidi-Ahy, and I.-J. Feng, "Propagation modes and dispersion characteristics of coplanar waveguides," *IEEE Trans. Microwave Theory Tech.*, Vol. 38, 245–251, 1990.
16. Heinrich, W, F. Schnieder, and T. Tischler, "Dispersion and radiation characteristics of conductor-backed CPW with finite ground width," *2000 IEEE MTT-S Int. Microwave Symp. Digest*, 1663–1666, 2000.
17. Pozar, D. M., *Microwave Engineering*, John Wiley and Sons, New York, 2005.
18. Fano, R. M., "Theoretical limitations of the broadband matching of arbitrary impedances," *J. Franklin Institute*, Vol. 429, 57–85, 139–154, 1950.
19. Abramowitz, M. and I. A. Stegun, *Handbook of Mathematical Functions*, Dover, New York, 1972.
20. Wang, S.-N. and N.-W Chen, "Compact, ultra-broadband coplanar-waveguide bandpass filter with excellent stopband rejection," *Progress In Electromagnetics Research B*, Vol. 17, 15–28, 2009.
21. Vinoy, K. J. and P. U. Reddy, "Design of narrowband bandpass

filter on coplanar waveguide using spiral slots," *Progress In Electromagnetics Research Letters*, Vol. 6, 139–148, 2009.

22. Chen, J., G. Fu, G.-D. Wu, and S.-X. Gong, "Compact graded central feeder line CPW-fed broadband antenna," *Journal of Electromagnetics Waves and Applications*, Vol. 23, Nos. 14–15, 2089–2097, 2009.
23. Chen, H., Y. H. Wu, Y. M. Yang, and Y. X. Zhang, "A novel and compact bandstop filter with folded microstrip/CPW hybrid structure," *Journal of Electromagnetics Waves and Applications*, Vol. 24, No. 1, 103–112, 2010.
24. Sze, J.-Y., T.-H. Hu, and T.-J. Chen, "Compact dual-band annular-ring slot antenna with meandered grounded strip," *Progress In Electromagnetics Research*, Vol. 95, 299–308, 2009.
25. Alkanhal, M. A. S., "Composite compact triple-band microstrip antennas," *Progress In Electromagnetics Research*, Vol. 93, 221–236, 2009.
26. Liao, W.-J., S.-H. Chang, and L.-K. Li, "A compact planar multiband antenna for integrated mobile devices," *Progress In Electromagnetics Research*, Vol. 109, 1–16, 2010.
27. Sze, J.-Y. and Y.-F. Wu, "A compact planar hexa-band internal antenna for mobile phone," *Progress In Electromagnetics Research*, Vol. 107, 413–425, 2010.
28. Malekabadi, S. A., A. R. Attari, and M. M. Mirsalehi, "Design of compact broadband microstrip antennas using coplanar coupled resonators," *Journal of Electromagnetic Waves and Applications*, Vol. 23, No. 13, 1755–1762, 2009.
29. Jaw, J.-L., F.-S. Chen, and D.-F. Chen, "Compact dualband CPW-fed slotted patch antenna for 2.4/5 GHz Wlan operation," *Journal of Electromagnetic Waves and Applications*, Vol. 23, No. 14–15, 1947–1955, 2009.
30. Powell, M. J. D. "A fast algorithm for nonlinearly constrained optimization calculations," *Lecture Notes in Mathematics*, Vol. 630, 144–157, 1978.